DALTON
FULL PAPER

Dinuclear ruthenium(II) complexes $[\{(L)ClRu^{II}\}_2(\mu\text{-tppz})]^{2+}$ (L = an arylazopyridine ligand) incorporating tetrakis(2-pyridyl)-pyrazine (tppz) bridging ligand: synthesis, structure and spectroelectrochemical properties

Nripen Chanda,[a] Rebecca H. Laye,[b] Soma Chakraborty,[a] Rowena L. Paul,[b] John C. Jeffery,[b] Michael D. Ward *[b] and Goutam Kumar Lahiri *[a]

[a] *Department of Chemistry, Indian Institute of Technology, Bombay, Powai, Mumbai-400076, India. E-mail: lahiri@ether.chem.iitb.ac.in*
[b] *School of Chemistry, University of Bristol, Cantock's Close, Bristol, UK BS8 ITS. E-mail: mike.ward@bristol.ac.uk*

Received 20th May 2002, Accepted 8th July 2002
First published as an Advance Article on the web 19th August 2002

A series of dinuclear complexes $[\{(L^{1-4})ClRu^{II}\}_2(\mu\text{-tppz})][ClO_4]_2$ {[**1**]$(ClO_4)_2$ to [**4**]$(ClO_4)_2$} has been prepared, in which two $\{Ru^{II}(L^{1-4})Cl\}^+$ fragments [L = a 2-arylazopyridine ligand of the type 2-(C_5H_4N)–N=N–C_6H_4R; for L^1, R = H; L^2, R = *p*-Me; L^3, R = *p*-Cl; L^4, R = *m*-Me] are linked by the bridging ligand tppz [2,3,5,6-tetrakis(2-pyridyl)pyrazine]. A single isomer forms during the synthesis in each case, and the crystal structure of [**4**]$(ClO_4)_2$ shows it to be a twofold-symmetric isomer with each ligand L arranged such that its pyridine donor is on the long axis of the molecule (*trans* to the pyrazine ring of tppz) and the azo donor is *trans* to one of the pyridyl donors of tppz. This allows the peripheral aryl ring attached to the azo unit of each ligand L to be oriented over either face of the bridging ligand giving a three-layer π-stacked (aryl–pyrazine–aryl) sandwich. Electrochemical studies revealed (i) separations of 190–250 mV (depending on the aryl substituent of L) between the successive Ru(II)/Ru(III) couples, indicative of a significant inter-metallic electronic coupling, and (ii) several ligand-based reductions of the π-acceptor pyrazine and arylazopyridine ligands. A UV/Vis/NIR spectroelectrochemical study showed the presence of an IVCT transition at *ca.* 1900 nm in MeCN for the Ru(II)–Ru(III) mixed-valence states, whose narrowness is indicative of borderline class III behaviour. Several reduced forms of the complexes were also spectroscopically characterised.

Introduction

The development of newer classes of dinuclear metal complex incorporating suitable bridging ligands which lead to the formation of stable mixed valence states has attracted considerable research interest in recent years.[1,2] This is primarily due to the relevance of such complexes to biological processes,[3] molecular electronics[4] and for theoretical studies on electron transfer kinetics.[5] The bridging ligand mediated intermetallic electronic communication takes place through their π-symmetry orbitals either by electron-transfer or hole-transfer mechanisms.[1]

Since the discovery of pyrazine-mediated strong intermetallic coupling in the Creutz–Taube complex,[6–8] interest has been built up in the direction of designing binuclear ruthenium(II) complexes incorporating polyazine based heterocyclic bridging ligands, such as 2,3-bis(2-pyridyl)aminoxaline,[9] 2,2′-bipyrimidine,[10] 2,3-bis(2-pyridyl)pyrazine,[11] tetrapyrido[2,3-*a*:3′,2′-*c*:2″,3″-*h*:3‴,2‴-*j*]phenazine[12] and 2,3,5,6-tetrakis(2-pyridyl)pyrazine (tppz).[13] The bis-tridentate tppz bridging function has been extensively used as a bridging ligand in recent years in combination with a wide variety of terminal ligands ranging in character from π-acidic (*e.g.* 2,2′-bipyridine, 2,2′:6′,2″-terpyridine) and σ-donor (monodentate amines) in order to prepare homo- or hetero-polynuclear ruthenium complexes.[13] In all cases, tppz has been found to be an effective mediator for intermetallic coupling almost of the order of the Creutz–Taube ion.[13]

Although the electronic nature of the bridging function plays the most crucial role in the intermetallic coupling process, the electronic properties of the peripheral co-ligands are also a factor in determing the degree of electronic coupling between the metal centres.[14] In view of this, the present work originated from our interest in synthesizing diruthenium-tppz complexes comprising very strongly π-acidic azopyridine $\{NC_5H_4–N=N–C_6H_4(R)\}$ terminal ligands, L. The azoimine (–N=N–C=N–) function of L is isoelectronic with the diimine (–N=C–C=N–) function of bipyridine (bpy), but the much stronger π-acidic nature of L makes its complexes a facile successive receptor of electrons in the low lying ligand-based LUMOs.[15] Therefore, polynuclear complexes having azopyridine derivatives as terminal ligands are expected to provide an additional opportunity to examine the spectroelectrochemical properties of the reduced forms of the complexes. Further, the incorporation of different substituents onto the aryl unit of the arylazopyridine ligands allows fine-tuning of their electronic properties.

Herein we report the synthesis of the four complexes $[\{(L^{1-4})ClRu^{II}\}_2(\mu\text{-tppz})]^{2+}$, [**1**]$(ClO_4)_2$–[**4**]$(ClO_4)_2$, including the crystal structure of one representative example, and the electrochemical and spectroscopic properties of the complexes including detailed spectroeletrochemical studies over a wide range of accessible oxidation states.

Results and discussion

Synthesis and characterisation of complexes

A group of four azo-imine based 2-arylazopyridine ligands L^1–L^4 has been used as the peripheral ligands for the present study. Ligands L^1–L^3 were chosen to provide a range of substituents with different properties attached to the *para*-position of the aryl unit, from electron-withdrawing (Cl substituent in L^3; Hammett parameter +0.30) to electron donating (methyl substituent in L^2; Hammett parameter −0.18). Ligand L^4 (with

 DOI: 10.1039/b204862k

Table 1 Microanalytical,[a] conductivity,[b] and EPR[c] data

Compound	Elemental anlysis (%) C	H	N	Λ_M/Ω^{-1} cm^2 mol^{-1}	g_{iso}	Peak width/G
[**1**]$(ClO_4)_2\cdot 2H_2O$	43.57 (43.82)	2.99 (2.83)	13.57 (13.33)	256	1.999	10
[**2**]$(ClO_4)_2\cdot 2H_2O$	45.39 (45.00)	3.09 (3.28)	13.41 (13.00)	250	1.996	10
[**3**]$(ClO_4)_2\cdot 2H_2O$	41.67 (41.51)	2.87 (2.73)	12.85 (12.64)	240	1.993	12.5
[**4**]$(ClO_4)_2\cdot 2H_2O$	45.42 (45.00)	3.33 (3.28)	12.78 (13.00)	245	1.999	10

[a] Calculated values are in parentheses. [b] In acetonitrile solution at 298 K. [c] In acetonitrile at 77 K.

the methyl substituent at the *meta* position of the aryl ring) is also included because it afforded a crystalline complex for X-ray analysis; for a comparison of electronic substituent effects, L^1–L^3 are more significant. The dinuclear complexes $[\{Cl(L)Ru^{II}\}_2(\mu\text{-tppz})]^{2+}$, $[\mathbf{1}]^{2+}$–$[\mathbf{4}]^{2+}$, were synthesized *via* the reaction of the appropriate ligand L with the precursor ruthenium complex $[Cl_3Ru^{III}(\mu\text{-tppz})Ru^{III}Cl_3]$, in the presence of NEt_3 and LiCl in refluxing EtOH medium under a dinitrogen atmosphere (Scheme 1). The complexes were isolated as

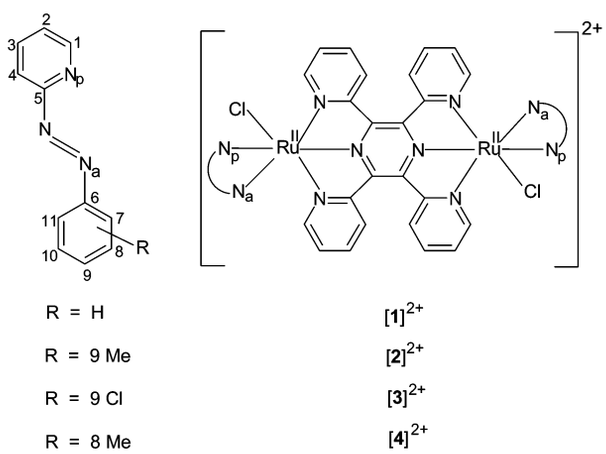

Scheme 1

their dihydrated perchlorate salts, $[\{Cl(L)Ru\}_2(\mu\text{-tppz})](ClO_4)_2\cdot 2H_2O$. The reaction in Scheme 1 also leads to the simultaneous formation of *ctc*-$[Ru(L)_2Cl_2]$ [*ctc* = *cis-trans-cis* with respect to chlorides, pyridine (N_p) and azo (N_a) nitrogens respectively][16] as a minor side product (yield is approximately 5%). The undesired *ctc*-$[Ru(L)_2Cl_2]$ products were separated from the respective complexes $\{[\mathbf{1}]^{2+}$–$[\mathbf{4}]^{2+}\}$, by column chromatography.

The unsymmetrical nature of L (arising from the inequivalence of the pyridine nitrogen, N_p, and the azo nitrogen, N_a) leads to the possibility of simultaneous formation of six geometrical isomers (**A**–**F**). However, only one such product was formed during the syntheses of each of the four complexes. The spectral features of the complexes $[\mathbf{1}]^{2+}$, $[\mathbf{2}]^{2+}$ and $[\mathbf{3}]^{2+}$ are akin to those of the structurally characterised complex $[\mathbf{4}]^{2+}$ (see below) making it logical to believe that all the four complexes exist in the same isomeric form. Similarly, for the analogous bipyridine derivative $[\{Cl(dmb)Ru\}_2(\mu\text{-tppz})]^{2+}$ (dmb = 4,4′-dimethyl-2,2′-bipyridine), the *trans*-isomer (*trans* with respect to two Ru–Cl bonds) was also obtained as a major product, although a minor product of a different isomer was also observed in this case.[13g]

The complexes exhibit satisfactory microanalytical data and conductivities in acetonitrile solution (Table 1). Further confirmation of the composition of the complexes were established from the positive ion electrospray mass spectrum of the representative complex $[\mathbf{4}](ClO_4)_2$ which showed a strong molecular ion peak centred at *m*/*z* 1157.0 corresponding to $\{[\mathbf{4}](ClO_4)\}^+$ (calculated molecular weight, 1155.03). The ionic perchlorate

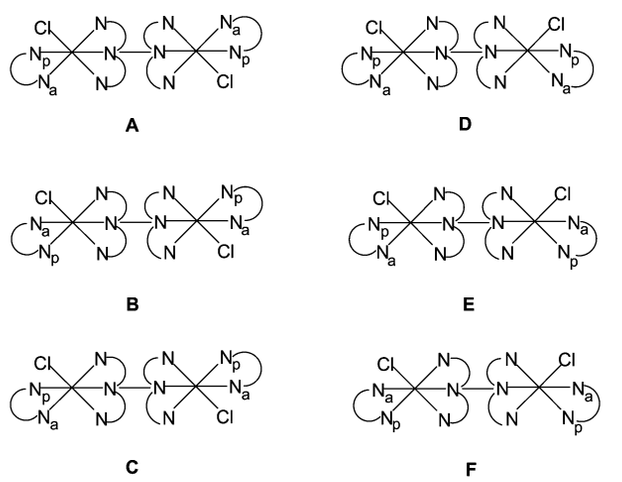

bands are obtained in the IR spectrum near 1100 and 625 cm^{-1}. The presence of a single Ru–Cl stretching frequency near 320 cm^{-1} is also consistent with a geometry in which both Ru–Cl bonds are equivalent, *i.e.* **A**, **B**, **D** or **F** (the two Ru–Cl bonds are far apart enough to ignore coupling between them such that each of these isomers is likely to give a single Ru–Cl vibration). The ^{1}H NMR spectrum of $[\mathbf{4}](ClO_4)_2\cdot 2H_2O$ in $(CD_3)_2SO$ (Fig. 1), is also in agreement with twofold symmetry

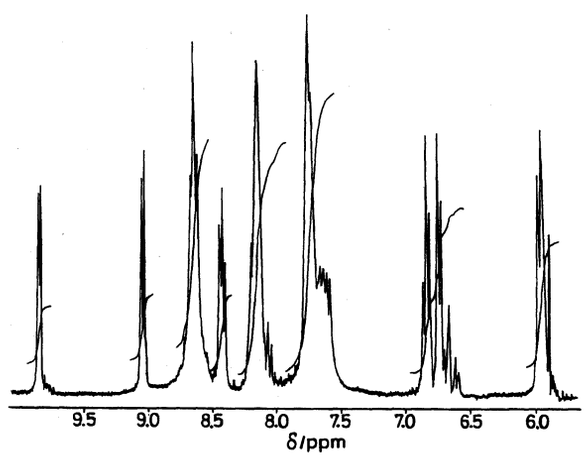

Fig. 1 ^{1}H NMR spectrum of $[\mathbf{4}](ClO_4)_2$ in $(CD_3)_2SO$ solvent.

in the complex molecule, exhibiting 16 aromatic protons: 8 from one *m*-tolyl-azopyridine (L^4) and eight from the two inequivalent pyridyl rings of the bridging tppz unit (overlapping between 6–10 ppm). The methyl signal of L^4 appears as a singlet at 1.9 ppm. Note that the presence of two equivalent Ru termini (from IR and NMR data) is again consistent with structures **A**, **B**, **D** or **F**.

The crystal structure of $[\mathbf{4}](ClO_4)_2$ is shown in Fig. 2 and unequivocally establishes the structure as **A**, with mutually '*trans*' chloride ligands, and the pyridyl donors of the terminal ligands both lying on the long axis of the complex. Selected bond distances and angles are listed in Table 2. The asymmetric

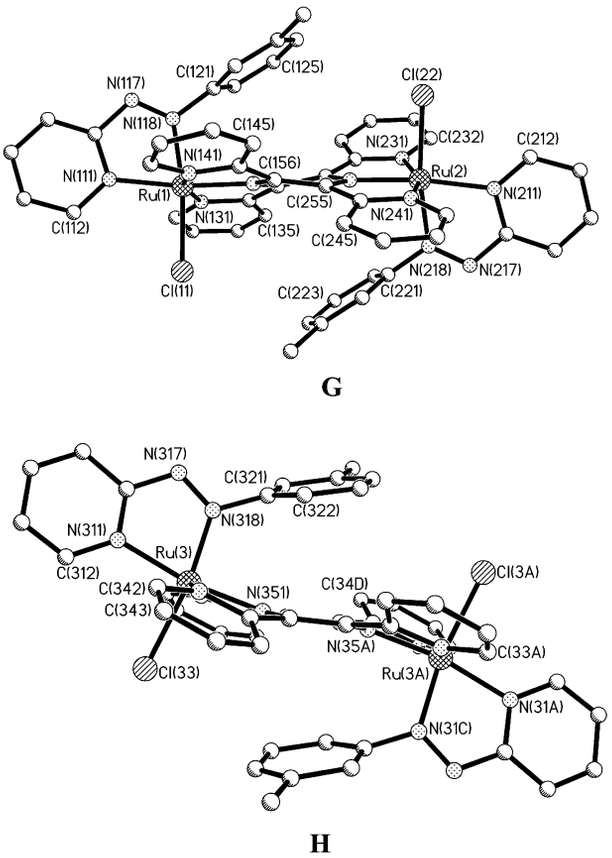

Fig. 2 Edge-on views of the two independent complex cations in the structure of $[4](ClO_4)_2 \cdot (H_2O)_{2/3} \cdot (CH_2Cl_2)_{1/3}$, emphasising (i) the conformation of the bridging ligand, and (ii) the aromatic stacking involving the aryl rings on the terminal ligands and the pyrazinyl unit of the bridging ligand.

unit contains two independent types of complex unit (**G** and **H**), one in a general position (**G**) and the other astride an inversion centre (**H**), such that the occupancy of the asymmetric unit is 1.5 complex molecules (plus one water molecule and half a molecule of dichloromethane).

In both types of complex (**G** and **H**), the Ru–Cl bonds are in a mutually *trans* configuration, with Cl ··· Cl separations of 8.173 and 8.792 Å respectively. The RuN_5Cl coordination sphere around each ruthenium centre is distorted octahedral, which is reflected in the *trans* angles of the meridionally coordinated tppz ligand: N(131)–Ru(1)–N(141), 160.1(14)°; N(231)–Ru(2)–N(241), 158.8(4)° and N(331)–Ru(3)– N(341), 158.4(4)°; these are comparable to the distortions from octahedral symmetry seen on other complexes of tppz.[13g,17,18] In both complex cations, it is clear that there is aromatic stacking between the pendant phenyl rings of the terminal arylazopyridine ligand and the central pyrazine ring of tppz; these phenyl rings, one from each end of the complex, lie above and below the central pyrazine ring to give a three-layer stack. The presence of this interaction may explain the presence of only a single isomer in each case: for the interaction to occur requires that the ligand L is coordinated with the pyridyl N atom on the molecular long-axis, such that the pendant aryl unit, directed off to one side, is available for stacking with the bridging ligand. In each case the pendant phenyl ring cannot manage to be parallel with the central pyrazine ring but is at an angle to it [for C(121)–C(126) in complex **G**, 30.7°; for C(221)–C(226) in complex **G**, 31.5°; for C(321)–C(326) in complex **H**, 23.7°]. Because of this divergence the inter-ring distances within the stacks (defined as the distances from the mean plane of the pyrazine ring to the individual atoms in the phenyl rings) accordingly span a wide range, of about 2.8–4.1 Å.

The major difference between units **G** and **H** is the conformation of the tppz ligand, which is substantially distorted from planarity in each case. In complex cation **G**, the tppz ligand is saddle-shaped such that a mutually *trans* pair of pyridyl substituents (*e.g.* at C^2 and C^5 of the pyrazine nucleus) are bent in the same sense towards one face of the pyrazine ring, whereas the other pair of pyridyl substituents (at C^3 and C^6) are bent in the opposite sense. This is shown by the offsets of the four carbon atoms C(136), C(236), C(246) and C(146) from the pyrazine mean plane; the values are +0.523, −0.556, +0.517 and −0.525 Å respectively, *i.e.* a regular alternation around the ring. A consequence of this is that the two RuN_3 planes involving the tppz ligand are substantially twisted with respect to one another, by 27.6°; this is also reflected in the angle between the mean planes of the terminal pyridyl rings of the arylazopyridine ligand, which instead of being zero, is 33.1°. In complex cation **H** in contrast, it is the two pyridine rings at the same end of the pyrazine bridge (*e.g.* attached to C^2 and C^6 of the pyrazine) which are offset towards the same face of the pyrazine ring, with the other pair of pyridines (at the C^3 and C^5 positions) directed towards the other face. Thus, the offsets of the carbon atoms C(336) and C(346) from the mean plane of the pyrazine ring are 0.202 and 0.225 Å (in the same sense) respectively, whereas in the other half of the complex the symmetry-equivalent pair of C atoms are offset by the same extent but in the opposite direction. The bridging ligand accordingly has a 'stepped' rather than a saddle-shaped structure, and the two RuN_3 mean planes are necessarily parallel although they are offset by 0.47 Å (Fig. 2). The Ru ··· Ru separations are 6.581 and 6.563 Å for **G** and **H** respectively.

The Ru–N(pyrazine) distances in **G** and **H**, Ru(1)–N(151), 1.965(9); Ru(2)–N(254), 1.941(8) and Ru(3)–N(351), 1.957(10) Å, match well with reported data for related complexes.[13g,17] The shortness of the Ru–N(pyrazine) distances as compared to the Ru–N(pyridine) distances within the tppz unit (Table 2) can be attributed to stronger back-bonding to the pyrazine unit compared to the pyridines. This reflects their relative abilities to act as π-acceptor units, and the effective d(π)–p(π) Ru-pyrazine overlap helps to provide the necessary pathway for the intermetallic electronic coupling.[19] A similar effect arises in the coordinated arylazopyridine ligands L^4, for which in every case the Ru–N(azo) distance is shorter than the Ru–N(pyridine) distance by *ca.* 0.1 Å, reflecting the stronger π-acidity of the azo unit. A consequence of this is that the average azo(N=N) distance [1.289(12) Å] of coordinated L^4 is significantly longer than that found in the free azo ligands (*ca.* 1.25 Å),[20] as also observed earlier in other complexes of arylazopyridines.[21] The average Ru–Cl distance of 2.390 (2) Å in $[4](ClO_4)_2$ compares well with other reported Ru^{II}–Cl distances.[13g,22]

Redox properties of the complexes

The redox properties of the complexes $[1]^{2+}$–$[4]^{2+}$ were studied by cyclic voltammetric and differential pulse voltammetric techniques in acetonitrile solution using a platinum working electrode. The complexes are electroactive with respect to the metal as well as the ligand centres and display multiple reversible redox processes in the potential range ±2 V *versus* SCE. Representative voltammograms are shown in Fig. 3 and redox potential data are given in Table 3.

All four complexes display two successive one-electron redox processes (couples I and II) in the range 1.28–1.59 V *versus* SCE, which are readily assigned as successive metal-centred Ru(II)/Ru(III) couples. The one-electron nature of the first process has been confirmed by constant-potential coulometry. The separation of *ca.* 200–250 mV between the Ru(II)/Ru(III) couples indicates a moderate intermetallic electronic coupling across the tppz bridging ligand, and corresponds to comproportionation constant (K_c) values in the range of 2.2×10^3–2.11×10^4 (Table 3) [using the equation $RT\ln K_c = nF(\Delta E)$] in

Table 2 Selected bond distances (Å) and angles (°) for $[4](ClO_4)_2 \cdot (H_2O)_{2/3} \cdot (CH_2Cl_2)_{1/3}$

Ru(1)–N(118)	1.960(7)	Ru(2)–Cl(22)	2.387(2)
Ru(1)–N(151)	1.965(9)	Ru(3)–N(318)	1.943(12)
Ru(1)–N(111)	2.045(9)	Ru(3)–N(351)	1.957(10)
Ru(1)–N(131)	2.073(10)	Ru(3)–N(311)	2.057(12)
Ru(1)–N(141)	2.085(9)	Ru(3)–N(331)	2.051(9)
Ru(1)–Cl(11)	2.384(2)	Ru(3)–N(341)	2.073(9)
Ru(2)–N(218)	1.963(7)	Ru(3)–Cl(33)	2.401(3)
Ru(2)–N(254)	1.941(8)	N(117)–N(118)	1.279(11)
Ru(2)–N(211)	2.064(9)	N(217)–N(218)	1.284(11)
Ru(2)–N(231)	2.065(9)	N(317)–N(318)	1.304(14)
Ru(2)–N(241)	2.057(9)		
N(118)–Ru(1)–N(151)	97.1(3)	N(254)–Ru(2)–N(218)	98.0(3)
N(118)–Ru(1)–N(111)	75.9(3)	N(254)–Ru(2)–N(241)	80.3(4)
N(151)–Ru(1)–N(111)	172.4(3)	N(218)–Ru(2)–N(241)	93.4(3)
N(118)–Ru(1)–N(131)	93.0(3)	N(254)–Ru(2)–N(211)	172.8(3)
N(151)–Ru(1)–N(131)	80.2(4)	N(218)–Ru(2)–N(211)	75.5(3)
N(111)–Ru(1)–N(131)	103.0(4)	N(241)–Ru(2)–N(211)	96.9(4)
N(118)–Ru(1)–N(141)	93.6(3)	N(254)–Ru(2)–N(231)	78.8(4)
N(151)–Ru(1)–N(141)	80.3(4)	N(218)–Ru(2)–N(231)	93.5(3)
N(111)–Ru(1)–N(141)	96.8(3)	N(241)–Ru(2)–N(231)	158.8(4)
N(131)–Ru(1)–N(141)	160.1(4)	N(211)–Ru(2)–N(231)	104.2(3)
N(118)–Ru(1)–Cl(11)	171.0(3)	N(254)–Ru(2)–Cl(22)	91.2(2)
N(151)–Ru(1)–Cl(11)	91.6(2)	N(218)–Ru(2)–Cl(22)	170.8(2)
N(111)–Ru(1)–Cl(11)	95.5(2)	N(241)–Ru(2)–Cl(22)	88.9(2)
N(131)–Ru(1)–Cl(11)	86.2(2)	N(211)–Ru(2)–Cl(22)	95.4(2)
N(141)–Ru(1)–Cl(11)	90.1(2)	N(231)–Ru(2)–Cl(22)	87.5(2)
N(318)–Ru(3)–N(351)	93.6(4)	N(331)–Ru(3)–N(341)	158.4(4)
N(318)–Ru(3)–N(331)	87.4(4)	N(311)–Ru(3)–N(341)	100.6(4)
N(351)–Ru(3)–N(331)	80.3(4)	N(318)–Ru(3)–Cl(33)	168.1(4)
N(318)–Ru(3)–N(311)	76.7(5)	N(351)–Ru(3)–Cl(33)	95.6(3)
N(351)–Ru(3)–N(311)	170.1(4)	N(331)–Ru(3)–Cl(33)	86.7(2)
N(331)–Ru(3)–N(311)	100.5(4)	N(311)–Ru(3)–Cl(33)	94.3(3)
N(318)–Ru(3)–N(341)	102.2(4)	N(341)–Ru(3)–Cl(33)	86.9(2)
N(351)–Ru(3)–N(341)	79.8(4)		

Table 3 Electrochemical data at 298 K[a]

	E^0_{298}/V (ΔE_p/mV)								ν_{MLCT}/cm^{-1}		
Compound	Couple I	Couple II	Couple III	Couple IV	Couple V	Couple VI	Couple VII	ΔE^b/V	Obs.[c]	Calc.[d]	K_c[e]
$[1]^{2+}$	1.28 (70)	1.51 (88)	−0.44 (70)	−0.81 (70)	−0.98 (70)	−1.43 (70)	−1.59 (150)	1.72	17452	16872	4.0×10^3
$[2]^{2+}$	1.32 (70)	1.58 (90)	−0.40 (60)	−0.81 (70)	−0.99 (70)	−1.42 (90)	−1.57 (80)	1.72	17271	16872	2.1×10^4
$[3]^{2+}$	1.40 (100)	1.59 (100)	−0.31 (70)	−0.67 (80)	−0.85 (60)	−1.34 (70)	−1.53 (80)	1.71	17331	16791	2.2×10^3
$[4]^{2+}$	1.29 (80)	1.52 (90)	−0.45 (80)	−0.83 (80)	−1.28 (100)	−1.43 (80)	−1.63 (110)	1.74	17361	17033	6.4×10^3

[a] Solvent, acetonitrile; supporting electrolyte, $[NEt_4][ClO_4]$; reference electrode, SCE; solute concentration, 10^{-3} mol dm^{-3}; working electrode, platinum wire; scan rate, 50 mVs^{-1}; $E^0_{298} = 0.5(E_{pa} + E_{pc})$ where E_{pa} and E_{pc} are cathodic and anodic peak potentials respectively. [b] Calculated using eqn. (2). [c] In acetonitrile. [d] Calculated using eqn. (1). [e] Calculated using the eqn. $RT\ln K_c = nF(\Delta E)$.

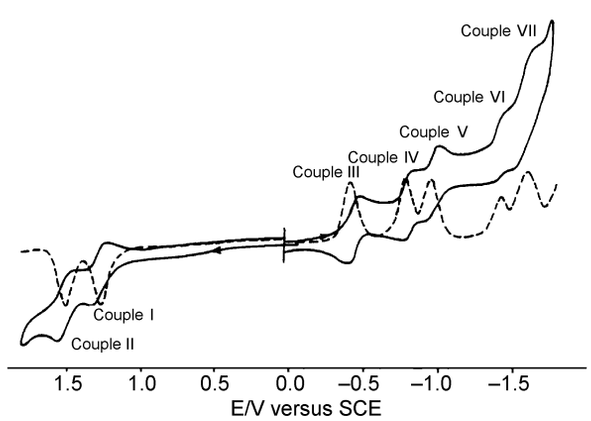

Fig. 3 Cyclic voltammograms and differential pulse voltammograms of $[1](ClO_4)_2$ in CH_3CN at a Pt working electrode (scan rate 50 mV s^{-1}).

the mixed valence states of $[1]^{3+}$–$[4]^{3+}$, indicative of class II mixed valence states.[23] The K_c value changes slightly depending on the nature and location of the 'R' groups present in the pendant phenyl ring of L. For the *para*-substituted ligand series, the K_c values follow the order $[3]^{3+} < [1]^{3+} < [2]^{3+}$, with the electron-withdrawing chloro-substituent giving the weakest coupling and electron-releasing methyl substituent giving the strongest coupling.

For comparison, the successive Ru(II)/Ru(III) couples of the analogous complex $[\{Cl(bpy)Ru^{II}\}_2(\mu\text{-tppz})]^{2+}$ (with terminal 2,2′-bipyridine ligands) appear at 0.96 and 1.25 V; compared to our new complexes, these redox potentials are less positive and also more substantially separated (290 mV).[13g] Therefore, due to the stronger π-acidic character of L compared to bpy, the potentials of the corresponding Ru(II)/Ru(III) couples in $[1]^{2+}$–$[4]^{2+}$ are positively shifted by approximately 0.3 V. Similarly, Ru(II)/Ru(III) potentials of $[1]^{2+}$–$[4]^{2+}$ are appreciably higher (about 150 mV) than those of the corresponding mononuclear mixed-ligand terpyridine-azopyridine complexes $[Cl(L)Ru(trpy)]^+$ (trpy = 2,2′:6′,2″-terpyridine), due to the stronger π-acceptor character of tppz relative to terpyridine.[22a] The more positive redox potentials in the arylazopyridine complexes are to be expected, but it is interesting to note that the reduction in electron density at the metal centres also results in a decrease in the electronic coupling between them. It is reasonable to suggest therefore that the overall reduction in metal-centred electron-density will decrease the extent to which the unpaired electron is delocalised across the bridging ligand in the mixed-

valence state. This is the same effect as was noted above for the different substituents, with the most electron-withdrawing substituent giving the smallest separation between the Ru(II)/Ru(III) couples.

Both arylazopyridine (L) and tppz ligands are well known to be redox-active. Each ligand can accommodate two electrons in the electrochemically accessible lowest unoccupied molecular orbitals (LUMOs).[13,21] In the case of L, the LUMO is believed to be dominated by the azo function.[22,24] Since the complexes contain one tppz and two L ligands, six successive one-electron reductions are therefore expected (in principle) for each complex. However, in practice, we have observed five successive one-electron reductions within the experimental potential limit (−2.0 V *versus* SCE, Table 3). The order in which the ligands are reduced may be determined by comparison with previously-reported complexes containing L and tppz.

The first reduction of tppz occurs at a potential several hundred mV less negative than the first reduction of free L (with R = H);[25,26] likewise, the first reduction of coordinated tppz in $[\{Cl(bpy)Ru^{II}\}_2(\mu\text{-tppz})]^{2+}$ occurs at a less negative potential (−0.5 V *versus* SCE)[13g] than that of the arylazopyridine ligand L^1 in $[Cl(L^1)(trpy)Ru^{II}]^+$ (*ca.* −0.8 V *versus* SCE).[22a] Accordingly we assign the first reduction of $[\mathbf{1}]^{2+}$–$[\mathbf{4}]^{2+}$ (couple III) as tppz-based in each case, and the absolute redox potential values for couple III are consistent with this assignment.[13a,b,h,g] The next two reductions in each case (couples IV and V) are assigned as stepwise reductions of the two terminal arylazopyridine ligands,[22a] with the separation between them arising from a moderate electronic interaction between the two ends of the complex; these processes are too close together to be assigned as a pair of reductions on a single ligand. With each of the three π-acceptor ligands now reduced once, the next reduction (couple VI) will be the second tppz-based reduction. Usually the successive reductions of a coordinated tppz are separated by only *ca.* 500 mV,[13g] whereas here the separation between couples III and VI is about one volt; this may be ascribed to the intervening reductions of the arylazopyridine ligands, such that the second tppz-based reduction is made more difficult by the accumulated negative charge on the complex. Finally, couple VII is the second reduction of one of the arylazopyridine ligands.

Electronic spectra and spectroelectrochemistry

(i) Oxidations. In acetonitrile, complexes $[\mathbf{1}]^{2+}$–$[\mathbf{4}]^{2+}$ exhibit four strong transitions in the UV/Vis region (Fig. 4, Table 4). The strong transitions in the UV region are ligand-centred π–π* processes. The visible region is dominated by an intense transition near 580 nm (with ε values of *ca.* 30,000 $dm^3\ mol^{-1}\ cm^{-1}$ in each case), having a low-energy shoulder at *ca.* 700 nm. Given that the lowest-energy MLCT transition must involve the ligand

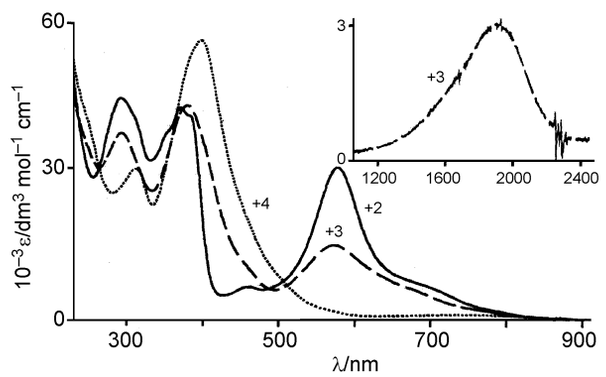

Fig. 4 Electronic spectra of $[\mathbf{3}]^{2+}$ (——), oxidised forms $[\mathbf{3}]^{3+}$ [Ru(II)–Ru(III) state, (---)] and $[\mathbf{3}]^{4+}$ [Ru(III)–Ru(III) state, (· · ·)], recorded in CH_3CN at 243 K during a spectroelectrochemical experiment. The inset shows the IVCT in the Ru(II)–Ru(III) state (with interference from solvent peaks subtracted).

Table 4 Electronic spectroscopic data for the complexes ($\mathbf{1}^{2+}$–$\mathbf{3}^{2+}$) in their different oxidation states, from spectroelectrochemical experiments (MeCN, 243 K)

Complex/charge	λ_{max}/nm ($10^{-3}\ \varepsilon$/dm^3 mol^{-1} cm^{-1})
$[\mathbf{1}](ClO_4)_2$	
+2	294 (43), 368 (36), 383 (36), 458 (7.0), 573 (31)[a]
+3	294 (39), 376 (41), 570 (14), 1890 (3.8)[b]
+4	313 (33), 397 (52), 748 (1.3)[c]
+1	313 (39), 388 (28), 567 (28), 868 (3.3), 992 (15)
0	316 (36), 368 (38), 567 (17), 990 (5.7)
−1	256 (34), 317 (37), 383 (51), 654 (17), 1149 (3.4)
$[\mathbf{2}](ClO_4)_2$	
+2	289 (42), 373 (42), 383 (40), 458 (6.9), 579 (30)[a]
+3	291 (35), 381 (41), 570 (10), 1890 (4.6)[b]
+4	312 (30), 399 (52), 748 (1.1)[c]
+1	315 (37), 387 (35), 571 (28), 875 (4.3), 996 (16)
0	377 (41), 570 (16), 990 (5.4)
−1	256 (33), 383 (47), 644 (16), 1133 (2.8)
$[\mathbf{3}](ClO_4)_2$	
+2	292 (44), 371 (42), 383 (41), 461 (6.8), 577 (31)[a]
+3	293 (37), 380 (43), 570 (15), 1890 (3.0)[b]
+4	313 (30), 398 (56), 740 (1.3)[c]
+1	314 (40), 387 (33), 570 (27), 870 (4.3), 984 (15)
0	308 (37), 378 (46), 636 (19), 990 (4.5)
−1	258 (33), 312 (34), 394 (49), 657 (16), 1144 (4.2)

[a] MLCT transition. [b] IVCT transition. [c] LMCT transition.

acceptor that is most easily reduced, this is assignable as a Ru[d(π)] ⟶ tppz(π*) MLCT transition.[13g] The predicted Ru[d(π)] ⟶ tppz(π*) MLCT energies for $[\mathbf{1}]^{2+}$–$[\mathbf{4}]^{2+}$, derived from the electrochemical data [eqns. (1) and (2)],[2b,27] agree well with the energies of these transitions observed in the electronic spectra (Tables 3 and 4).

$$\nu_{(MLCT)} = 8065(\Delta E_{1/2}) + 3000 \quad (1)$$

$$\Delta E_{1/2} = E_{1/2}(Ru^{III}\text{–}Ru^{II}) - E_{1/2}(tppz) \quad (2)$$

where $E_{1/2}$ (Ru^{III}–Ru^{II}) is the formal potential (in V) of the first reversible Ru(II)/Ru(III) couple (couple I); $E_{1/2}$(tppz) is the first tppz-based reduction; and $\nu_{(MLCT)}$ is the predicted wavenumber of the charge-transfer band in cm^{-1}.

We would also expect to see in the visible region the Ru[d(π)] ⟶ L(π*) MLCT transitions associated with the arylazopyridine π-acceptor ligands; on the basis of the electrochemical measurements, which shows that L is more difficult to reduce than tppz, these transitions are expected to be at higher energy than the 580 nm MLCT transition. In $[Cl(L)(trpy)Ru^{II}]^+$ for example the MLCT transition to the arylazopyridine occurs at *ca.* 510–520 nm, depending on the substituent, and has an intensity of 5,000–10,000 $dm^3\ mol^{-1}\ cm^{-1}$ (for a single chromophore).[22a] On this basis it is possible that the Ru[d(π)] ⟶ L(π*) MLCT transitions may overlap with the high-energy side of the Ru[d(π)] ⟶ tppz(π*) MLCT transition and not be separately resolved; evidence for this comes from the spectroelectrochemical studies (see below).

UV/Vis/NIR spectroelectrochemical measurements were performed on complexes $[\mathbf{1}]^{2+}$–$[\mathbf{3}]^{2+}$ in MeCN at 243 K over a range of six oxidation states, spanning charges −1 to +4. The results are summarised in Table 4 and Figs. 4 and 5; all of the complexes behaved very similarly, so the main points will be discussed with reference to complex $[\mathbf{3}]^{2+}$ whose spectra are used in the figures. On one-electron oxidation to $[\mathbf{3}]^{3+}$, giving the Ru(II)–Ru(III) mixed-valence state, there are two important changes in the electronic spectrum. Firstly, the intensity of the intense MLCT manifold in the visible region is reduced by

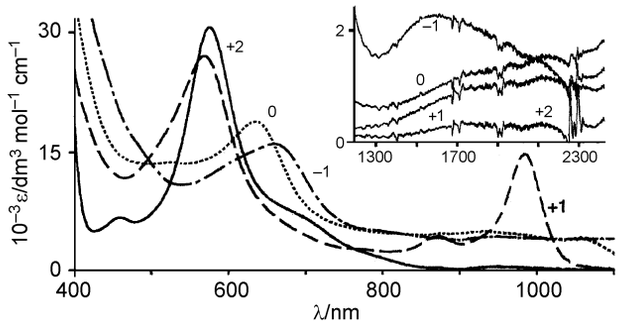

Fig. 5 Electronic spectra of $[\mathbf{3}]^{2+}$ (——), and the reduced forms $[\mathbf{3}]^{+}$ (---), $[\mathbf{3}]^{0}$ (· · ·) and $[\mathbf{3}]^{-}$ (- · -), recorded in CH_3CN at 243 K during a spectroelectrochemical experiment.

approximately 50%, consistent with the fact that the oxidised Ru centre is no longer acting as a π-donor. Actually we might expect a weak LMCT transition associated with the Ru(III) terminus to appear,[2f,28] but unless there is a strongly polarisable ligand in the donor set, it will be weak and any such transition will be obscured by the low-energy tail of the residual Ru(II)-centred MLCT transition. Secondly, a new low-energy transition at 1890 nm (ε = 3000 dm^3 mol^{-1} cm^{-1}) appears which is an inter-valence charge-transfer (IVCT) transition between the Ru(II) and Ru(III) termini. This transition is narrow, with a full-width at half maximum height (fwhm) value of 1650 cm^{-1}; it is also noticeably asymmetric, being cut off much more sharply on the low-energy side.[1i] For a Gaussian IVCT peak in a class II mixed-valence complex, with an absorption maximum at 5300 cm^{-1} the fwhm value is expected to be about 3500 cm^{-1}. This indicates the onset of class III behaviour, which means use of the Hush equation[29,30] to derive the electronic coupling constant V_{ab} from the parameters of the IVCT transition will produce an underestimate which can be considered as a lower limit. In fact application of the Hush equation gives V_{ab} values of *ca.* 510 cm^{-1} for $[\mathbf{3}]^{3+}$, 530 cm^{-1} for $[\mathbf{1}]^{3+}$ and 570 cm^{-1} for $[\mathbf{2}]^{3+}$. Based on the uncertainty in measurements from these near-IR transitions due to interference from solvent bands on the low-energy side we estimate an uncertainty in these values of *ca.* 10% which makes them more or less comparable although we note that order of V_{ab} values follows the order of K_c values for the mixed-valence states derived form electrochemical data, with $[\mathbf{2}]^{3+}$ having the largest and $[\mathbf{3}]^{3+}$ having the smallest.

There is very little literature data available to use for comparison purposes. Sauvage, Launay and co-workers[13a] calculated a V_{ab} value of *ca.* 3200 cm^{-1} for $[\{(\text{tterpy})\text{Ru}\}_2(\mu\text{-dppz})]^{5+}$ [tterpy = 4′-(tolyl)terpyridine] based on the assumption that it was class III, such that V_{ab} is just half the energy of the IVCT transition (a similar assumption for $[\mathbf{1}]^{3+}$–$[\mathbf{3}]^{3+}$ would give V_{ab} values of about 2600 cm^{-1} in each case, which we can take as an upper limit). The separation of 300 mV between the successive Ru(II)/Ru(III) couples for $[\{(\text{tterpy})\text{Ru}\}_2(\mu\text{-dppz})]^{5+}$ is however somewhat greater than we observe for $[\mathbf{1}]^{2+}$–$[\mathbf{4}]^{2+}$ over the same metal–metal separation, suggesting that $[\{(\text{tterpy})\text{Ru}\}_2(\mu\text{-dppz})]^{5+}$ should have a higher V_{ab}. The closest analogue to our complexes is $[\{\text{Cl(bpy)Ru}\}_2(\mu\text{-tppz})]^{2+}$ for which a redox separation of 290 mV between the Ru(II)/Ru(III) couples was measured but whose mixed-valence properties have not yet been fully described,[13g] although they are briefly mentioned in a recent review.[1i] In this review it is suggested that $[\{\text{Cl(bpy)Ru}\}_2(\mu\text{-tppz})]^{2+}$, which has a narrow IVCT transition at 6070 cm^{-1} (1647 nm), is best described as being electronically localised, although the narrowness of its IVCT transition implies decoupling of the inter-valence electron transfer from solvent reorientation.[1i] This happens when the rate of electron exchange in the (localised) mixed-valence state is sufficiently fast that the solvent reorientation cannot keep up and solvent averaging occurs, with the consequence that an electronically localised complex can still show the lack of solvent-dependence (and narrow IVCT transitions) more usually associated with class III behaviour. Such cases have been defined as class II–III hybrids.[1i] This seems to be an appropriate description for $[\mathbf{1}]^{3+}$–$[\mathbf{4}]^{3+}$, for which the separations between Ru(II)/Ru(III) redox potentials of up to 250 mV are less than the values often observed for genuine class III complexes (*e.g.* 390 mV for the Creutz–Taube ion),[6,7] but for which the IVCT transition is much narrower than expected for class II behaviour. Determination of V_{ab} values for these complexes is problematic because the simple assumptions used for class II or class III extremes give under- and over-estimates of V_{ab}, respectively, as shown above.[1i] It is noteworthy that the apparently very similar complex $[\{\text{Cl(bpy)}_2\text{Ru}\}_2(\mu\text{-pz})]^{4+}$ (pz = pyrazine), which has the same bridging pathway as in $[\{\text{Cl(dmb)Ru}\}_2(\mu\text{-tppz})]^{2+}$ and an essentially identical (pyridine)$_4$(pyrazine)(chloride) donor set, nonetheless has quite different electronic properties with a separation between Ru(II)/Ru(III) couples of only 120 mV.[31] This implies that it is not safe to use the data available for pyrazine-bridged mixed-valence complexes[1g] to compare with those containing a tppz bridge such as $[\mathbf{1}]^{2+}$–$[\mathbf{4}]^{2+}$, even when the donor sets are apparently very similar.

On further oxidation to the Ru(III)–Ru(III) state, the residual Ru(II)-centred MLCT transition disappears completely (Fig. 4), being replaced by a relatively weak transition at *ca.* 740 nm (ε, *ca.* 1000 dm^3 mol^{-1} cm^{-1}) which we assign as an LMCT process associated with the Ru(III) centres.[2f,28] Also the transition at 1890 nm disappears in every case, which confirms its assignment as an IVCT process since it is associated only with the mixed-valence state and not with either of the isovalent states.

(ii) Reductions. On one-electron reduction of each of the starting complexes to the +1 species, a reduction of the tppz bridging ligand ocurs resulting in one intense new transition at *ca.* 990 nm (ε, *ca.* 15000 dm^3 mol^{-1} cm^{-1}) in every case (Fig. 5). Given that the reduction is tppz-centred there are only two possibilities for this: (i) it could be an internal transition associated with the ligand radical, or (ii) it could be a ligand–ligand charge-transfer $[(\text{tppz}^{\bullet-}) \longrightarrow \text{L}(\pi^*)]$ from the now electron-rich ligand anion to the LUMO of one of the arylazopyridine π-acceptors. In the absence of any literature data on the electronic spectra of tppz-based radicals we can turn to calculations, and a ZINDO calculation shows that reduction of free tppz to its radical anion should generate an intense new electronic transition at 1010 nm (ε, 20000 dm^3 mol^{-1} cm^{-1}) which is a fully allowed π(SOMO) ⟶ π*(LUMO + 1) transition. This is in very good agreement with what we observe. Secondly, charge-transfer transitions between electron-rich and electron-deficient ligands have been demonstrated in related cases and tend to occur in the near-IR region of the spectrum.[32] It is perhaps surprising that the intensity of the principal MLCT transition at around 570 nm should only decrease in intensity by about 10% as the tppz unit is reduced; presumably this area of the spectrum (as suggested above) also includes the expected Ru[d(π)] ⟶ L(π*) MLCT transitions whose intensity will not be affected much by a tppz-based reduction.

Further reductions of the complexes to the neutral and then −1 states, *i.e.* reduction of each of the arylazopyridine ligands in turn according to the assignments discussed earlier, have two effects on the spectra (Fig. 5). Firstly, the area of MLCT absorption in the visible region (500–700 nm) steadily decreases in intensity as the ligand-based acceptor orbitals become singly occupied. Secondly, changes in the near-IR region, where ligand-radical centred and LLCT transitions are expected, occur. The intense transition at 992 nm discussed above almost completely disappears on reduction; this behaviour is not consistent with it being a solely tppz-radical centred transition, but suggests that it has $[(\text{tppz}^{\bullet-}) \longrightarrow \text{L}(\pi^*)]$ LLCT character which would be diminished by reduction of the acceptor ligands L. Also, in the +1, 0 and −1 states the near-IR region from 1200 nm downwards contains poorly-resolved broad areas

of absorbance which could be assigned to LLCT bands between reduced and non-reduced ligands, or to ligand-centred transitions associated with the radical states, or a combination of both.[32] For example, $[Ru(bpy)_3]^{2+}$ displays, in its partially-reduced forms, transitions in the region of 2000 nm associated with $(bpy^{\bullet -}) \longrightarrow (bpy)$ LLCT processes.[32d] Examination of the more highly reduced states of the complexes proved not to be possible due to slow decomposition of the complexes on the slow timescale of spectroelectrochemistry.

Finally, we note that the mono-reduced species $[\mathbf{1}]^+$–$[\mathbf{4}]^+$ could be generated on a larger scale from the starting complexes, either by controlled-potential coulometry in acetonitrile, or chemically by reduction with hydrazine hydrate in acetonitrile. The resulting violet-coloured solutions are reasonably stable at 298 K, although attempts to isolate the reduced species invariably resulted in re-oxidation during the work up process. Solutions of $[\mathbf{1}]^+$–$[\mathbf{4}]^+$ exhibit an intense, symmetric and sharp EPR signal at around $g = 2.0$ (see Table 1 for precise values), with a peak–peak separation of 10 G (Fig. 6); this signal is clearly indicative of formation of a ligand centred radical, as expected.[2b,33]

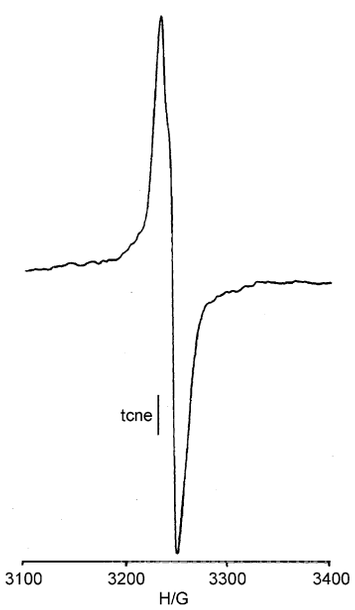

Fig. 6 X-Band EPR spectrum of chemically reduced complex $[\mathbf{4}]^+$ in CH_3CN solution at 77 K.

Conclusions

The series of dinuclear complexes described in this paper illustrate several points. The use of strongly π-acceptor terminal ligands (arylazopyridines, instead of *e.g.* bipyridine) shifts the Ru(II)/Ru(III) redox potentials to more positive values, as expected, and also decreases the K_c value for the mixed-valence Ru(II)–Ru(III) state [*i.e.* reduces the separation between the successive Ru(II)/Ru(III) couples]. Similar behaviour is seen on a smaller scale within the series of complexes with different substituents; an electron-donating substituent (methyl) on the aryl group of the terminal ligand slightly increases the K_c value, whereas an electron-withdrawing substituent (Cl) decreases it. Nevertheless, the redox separations of 190–250 mV indicate a still-substantial electronic coupling between the metal centres across the pyrazine-based bridging ligand. On one-electron oxidation to the Ru(II)–Ru(III) state all the complexes show an IVCT transition at *ca.* 1900 nm, which is in each case much narrower than expected for a class II mixed-valence state; this is indicative of some class III character, in agreement with the properties of two related complexes in the literature. Several ligand-centred reductions were also detected electrochemically, and electronic spectra of the reduced forms were recorded.

Experimental

Materials

The starting ruthenium precursor $[Cl_3Ru^{III}(\mu\text{-tppz})Ru^{III}Cl_3]$ was prepared according to the reported procedure.[13g] The peripheral 2-(arylazo)pyridine ligands (L^1–L^4) were synthesized using the literature methods.[16] Other chemicals and solvents were reagent grade and used as received. For electrochemical studies HPLC grade acetonitrile was used. Commercial tetraethyl ammonium bromide was converted to pure tetraethylammonium perchlorate (TEAP, used as base electrolyte) by following an available procedure.[34]

Physical measurements

Solution electrical conductivity was checked using a Systronic conductivity bridge 305. Infrared spectra were taken on a Nicolet spectrophotometer with samples prepared as KBr pellets. NMR spectrum was recorded in $(CD_3)_2SO$ solvent using a 300 MHz Varian FT spectrometer. UV/Vis/NIR spectroelectrochemical studies were performed in MeCN solvent at 243 K using an optically transparent thin layer electrode (OTTLE) cell mounted in the sample compartment of a Perkin-Elmer Lambda 19 spectrophotometer; the cell design and the method used have been described previously.[35] Cyclic voltammetric and coulometric measurements were carried out using a PAR model 273A electrochemistry system. A platinum wire working electrode, a platinum wire auxiliary electrode and a saturated calomel reference electrode (SCE) were used in a standard three-electrode configuration. TEAP was the supporting electrolyte and the solution concentration was *ca.* 10^{-3} mol dm^{-3}; the scan rate used was 50 mV s^{-1}. A platinum gauze working electrode was used in coulometric experiments. All electrochemical experiments were carried out under dinitrogen atmosphere and all redox potentials are uncorrected for junction potentials. The elemental analyses were carried out with a Perkin-Elmer 240C elemental analyser. The electrospray mass spectrum was recorded on a Finnigan LCQ ADVANTAGE mass spectrometer; USA.

Preparation of complexes [1–4](ClO$_4$)$_2$·2H$_2$O

All the complexes were prepared by the same general procedure, yields vary in the range 75–80%. The details are given for one representative complex, $[\mathbf{4}](ClO_4)_2\cdot 2H_2O$.

$[\{(L^4)ClRu^{II}\}_2(\mu\text{-tppz})](ClO_4)_2\cdot 2H_2O$, $[\mathbf{4}](ClO_4)_2\cdot 2H_2O$. The starting ruthenium complex $[Cl_3Ru^{III}(\mu\text{-tppz})Ru^{III}Cl_3]$ (150 mg, 0.19 mmol), L^4 (93 mg, 0.47 mmol), LiCl (80 mg, 1.9 mmol) and NEt_3 (0.5 cm^3) were added in absolute ethanol (20 cm^3) and the reaction mixture was heated to reflux with stirring for 6 h, under a dinitrogen atmosphere. The initial light green colour solution gradually changed to deep blue. The solvent was evaporated under reduced pressure. Saturated aqueous $NaClO_4$ solution was then added to the concentrated acetonitrile solution of the product. The solid precipitate thus obtained was filtered and washed thoroughly by cold ethanol followed by ice-cold water. The crude product was purified by column chromatography on alumina. Initially the side product $Ru(L^4)_2Cl_2$ was eluted using 5 : 1 CH_2Cl_2–CH_3CN; then the complex $[\mathbf{4}](ClO_4)_2\cdot 2H_2O$ was eluted using 5 : 2 CH_2Cl_2–CH_3CN mixture as eluent. Yield: 70% (170 mg). λ_{max}/nm (10^{-3} ε/dm^3 mol^{-1} cm^{-1}): 576 (33), 384 (46), 292 (49), 213 (104).

Crystallography

A small single crystal of $[\mathbf{4}](ClO_4)_2\cdot(H_2O)_{2/3}\cdot(CH_2Cl_2)_{1/3}$ was grown by slow diffusion of an acetonitrile solution of the

Table 5 Crystallographic data for [**4**]$(ClO_4)_2 \cdot (H_2O)_{2/3} \cdot (CH_2Cl_2)_{1/3}$

Empirical formula	$C_{48.33}H_{40}Cl_{4.67}N_{12}O_{8.67}Ru_2$
FW	1295.16
Crystal symmetry, space group	Triclinic, $P\bar{1}$
a/Å	10.9908(3)
b/Å	12.7354(3)
c/Å	27.5708(7)
α/°	98.012(2)
β/°	96.645(10)
γ/°	99.560(2)
V/Å^3	3730.10(16)
Z	3
T/K	90(2)
ρ_{calcd}/g cm^{-3}	1.730
Absorption coefficient/mm^{-1}	7.818
Data, restraints, parameters	7425, 24, 978
Final R_1, wR_2	0.0566, 0.2097

complex into benzene, followed by slow evaporation. Significant crystal data collection and refinement parameters are listed in Table 5. X-Ray measurements were made at 90 K using a Bruker-AXS Proteum area-detector diffractometer with monochromated Cu-Kα radiation (λ = 1.54056 Å). After integration of the raw data and merging of equivalent reflections, an absorption correction was applied based on comparison of multiple symmetry-equivalent measurements.[36] The structure was solved by direct methods and refined by full-matrix least squares on weighted F^2 values for all reflections using the SHELX suite of programs.[37] Most of the non-hydrogen atoms were assigned anisotropic displacement parameters and refined without positional constraints; however, due to the weakness of the data (the crystal was ≤ 0.1 mm in every dimension), 13 of the non-H atoms (the C atom of the disordered CH_2Cl_2 molecule, and 12 ligand C or N atoms) were refined isotropically to keep the refinement stable. All hydrogen atoms were constrained to ideal geometries and refined with fixed isotropic displacement parameters. Hydrogen atoms were not included for disordered solvent molecules, *viz.* two H_2O (each with 50% site occupancy) and one CH_2Cl_2 (with 50% site occupancy) per asymmetric unit. The main residual electron-density peaks, of around 1 e Å^{-3}, are in the vicinity of the partial-occupancy CH_2Cl_2 molecule and the nearby perchlorate anion, indicative of further disorder which could not be resolved

CCDC reference number 186198.

See http://www.rsc.org/suppdata/dt/b2/b204862k/ for crystallographic data in CIF or other electronic format.

Acknowledgements

Financial support received from the Council of Scientific and Industrial Research, New Delhi (India), the EPSRC (UK), and the Leverhulme Trust (UK) is gratefully acknowledged. Special acknowledgement is made to Regional Sophisticated Instrumentation Centre, RSIC, Indian Institute of Technology, Bombay, for providing NMR and EPR facilities.

References and notes

1 Reviews: (*a*) W. Kaim, A. Klein and M. Glöckle, *Acc. Chem. Res.*, 2000, **33**, 755; (*b*) J. A. McCleverty and M. D. Ward, *Acc. Chem. Res.*, 1998, **31**, 842; (*c*) D. Astruc, *Acc. Chem. Res.*, 1997, **30**, 383; (*d*) M. D. Ward, *Chem. Soc. Rev.*, 1995, **24**, 121; (*e*) R. J. Crutchley, *Adv. Inorg. Chem.*, 1994, **41**, 273; (*f*) G. Giuffrida and S. Campagna, *Coord. Chem. Rev.*, 1994, **135–136**, 517; (*g*) C. Creutz, *Prog. Inorg. Chem.*, 1983, **30**, 1; (*h*) W. Kaim, *Coord. Chem. Rev.*, 2002, **230**, 126; (*i*) K. D. Demandis, C. M. Hartshorn and T. J. Meyer, *Chem. Rev.*, 2001, **101**, 2655.

2 Recent examples: (*a*) S. Chakraborty, R. H. Laye, R. L. Paul, R. G. Gonnade, V. G. Puranik, M. D. Ward and G. K. Lahiri, *J. Chem. Soc., Dalton Trans.*, 2002, 1172; (*b*) B. Sarkar, R. H. Laye, B. Mondal, S. Chakraborty, R. L. Paul, J. C. Jeffery, V. G. Puranik, M. D. Ward and G. K. Lahiri, *J. Chem. Soc., Dalton Trans.*, 2002, 2097; (*c*) S. Chakraborty, R. H. Laye, P. Munshi, R. L. Paul, M. D. Ward and G. K. Lahiri, *J. Chem., Soc. Dalton Trans.*, 2002, 2348; (*d*) P. Passaniti, W. R. Browne, F. C. Lynch, D. Hughes, M. Nieuwenhuyzen, P. James, M. Maestri and J. G. Vos, *J. Chem. Soc., Dalton Trans.*, 2002, 1740; (*e*) P. J. Mosher, G. P. A. Yap and R. J. Crutchley, *Inorg. Chem.*, 2001, **40**, 1189; (*f*) R. H. Laye, S. M. Couchman and M. D. Ward, *Inorg. Chem.*, 2001, **40**, 4089; (*g*) W. E. Meyer, A. J. Amoroso, C. R. Horn, M. Jaeger and J. A. Gladysz, *Organometallics*, 2001, **20**, 1115; (*h*) J. E. Ritchie and R. W. Murray, *J. Am. Chem. Soc.*, 2000, **122**, 2964; (*i*) T. Weyland, K. Coustas, L. Toupet, J. F. Halet and C. Lapinte, *Organometallics*, 2000, **19**, 4228; (*j*) J.-P. Launay, S. Fraysse and C. Coudret, *Mol. Cryst., Liq. Cryst.*, 2000, **344**, 125; (*k*) S. Baitalik, U. Florke and K. Nag, *J. Chem. Soc., Dalton Trans.*, 1999, 719.

3 E. I. Solomon, T. C. Brunold, M. I. Davis, J. N. Kemsley, S. K. Lee, N. Lehnert, F. Neese, A. J. Skulan, Y. S. Yang and J. Zhou, *Chem. Rev.*, 2000, **100**, 235.

4 (*a*) F. Paul and C. Lapinte, *Coord. Chem. Rev.*, 1998, **178–180**, 431; (*b*) M. D. Ward, *Chem. Ind.*, 1996, 568; (*c*) M. D. Ward, *Chem. Ind.*, 1997, 640.

5 (*a*) B. S. Brunschwig and N. Sutin, *Coord. Chem. Rev.*, 1999, **187**, 233; (*b*) A. Bencini, I. Ciofini, C. A. Daul and A. Ferretti, *J. Am. Chem. Soc.*, 1999, **121**, 11418.

6 C. Creutz and H. Taube, *J. Am. Chem. Soc.*, 1969, **91**, 3988.

7 C. Creutz and H. Taube, *J. Am. Chem. Soc.*, 1973, **95**, 1086.

8 U. Furholz, S. Joss, H. B. Burgi and A. Ludi, *Inorg. Chem.*, 1985, **24**, 943.

9 D. P. Rillema, D. G. Taghdiri, D. S. Jones, C. D. Keller, L. A. Wori, T. J. Meyer and H. A. Levy, *Inorg. Chem.*, 1987, **26**, 578.

10 (*a*) J. D. Petersen, W. R. Murphy, Jr., R. Sahai, K. Brewer and R. R. Ruminski, *Coord. Chem. Rev.*, 1985, **64**, 261; (*b*) E. V. Dose and L. J. Wilson, *Inorg. Chem.*, 1978, **17**, 2660; (*c*) M. Hunziker and A. Ludi, *J. Am. Chem. Soc.*, 1977, **99**, 7370; (*d*) R. R. Ruminski and J. D. Petersen, *Inorg. Chem.*, 1982, **21**, 3706.

11 (*a*) C. H. Braunstein, A. D. Baker, T. C. Strekas and H. D. Gafney, *Inorg. Chem.*, 1984, **23**, 857; (*b*) R. R. Ruminski, T. Cockroft and M. Shoup, *Inorg. Chem.*, 1988, **27**, 4026; (*c*) V. Balzani, A. Juris, M. Venturi, S. Campagna and S. Serroni, *Chem. Rev.*, 1996, **96**, 759; (*d*) S. Serroni, S. Campagna, G. Denti, T. E. Keyes and J. G. Vos, *Inorg. Chem.*, 1996, **35**, 4513.

12 (*a*) A. Gourdon and J.-P. Launay, *Inorg. Chem.*, 1998, **37**, 5336; (*b*) P. Bonhote, A. Lecas and E. Amouyal, *Chem. Commun.*, 1998, 885.

13 (*a*) J. P. Collin, P. Laine, J. P. Launay, J. P. Sauvage and A. Sour, *J. Chem. Soc. Chem., Commun.*, 1993, 434; (*b*) C. R. Arana and H. D. Abruna, *Inorg. Chem.*, 1993, **32**, 194; (*c*) R. P. Thummel and S. Chirayil, *Inorg. Chim. Acta*, 1988, **154**, 77; (*d*) L. M. Vogler, B. Scott and K. J. Brewer, *Inorg. Chem.*, 1993, **32**, 898; (*e*) J. -D. Lee, L. M. Vrana, E. R. Bullock and K. J. Brewer, *Inorg. Chem.*, 1998, **37**, 3575; (*f*) T. S. Akasheh, D. Marji and Z. M. Al-Ahmed, *Inorg. Chim. Acta*, 1988, **141**, 125; (*g*) C. M. Hartshorn, N. Daire, V. Tondreau, B. Loeb, T. J. Meyer and P. S. White, *Inorg. Chem.*, 1999, **38**, 3200; (*h*) L. M. Vogler and K. J. Brewer, *Inorg. Chem.*, 1996, **35**, 818; (*i*) R. Ruminski, J. Kiplinger, T. Cockroft and C. Chase, *Inorg. Chem.*, 1989, **28**, 370.

14 S. Chellamma and M. Lieberman, *Inorg. Chem.*, 2001, **40**, 3177.

15 B. K. Santra and G. K. Lahiri, *J. Chem. Soc., Dalton Trans.*, 1997, 129 and references therein.

16 R. Samanta, B. Mondal, P. Munshi and G. K. Lahiri, *J. Chem. Soc., Dalton Trans.*, 2001, 1827.

17 V. Jondreau, A. M. Leiva, B. Loeb, D. Boys, L. K. Stultz and T. J. Meyer, *Polyhedron*, 1996, **15**, 2035.

18 M. Graf, B. Greaves and H. Stoeckli-Evans, *Inorg. Chim. Acta*, 1993, **204**, 239.

19 B. J. Coe, T. J. Meyer and P. S. White, *Inorg. Chem.*, 1995, **34**, 593.

20 (*a*) A. Mostad and C. Romming, *Acta Chem. Scand.*, 1971, **25**, 3561; (*b*) C. H. Chang, R. F. Porter and S. H. Bauer, *J. Am. Chem. Soc.*, 1970, **92**, 5313; (*c*) S. P. Sengupta and T. Roy, *Cryst. Struct. Commun.*, 1980, **9**, 965.

21 (*a*) B. K. Santra, G. A. Thakur, P. Ghosh, A. Pramanik and G. K. Lahiri, *Inorg. Chem.*, 1996, **35**, 3050; (*b*) N. Bag, A. Pramanik, G. K. Lahiri and A. Chakravorty, *Inorg. Chem.*, 1992, **31**, 40; (*c*) S. Goswami, A. R. Chakravarty and A. Chakravorty, *Inorg. Chem.*, 1983, **22**, 602; (*d*) R. A. Krause and K. Krause, *Inorg. Chem.*, 1982, **21**, 1714; (*e*) A. K. Deb, P. C. Paul and S. Goswami, *J. Chem. Soc., Dalton Trans.*, 1988, 2051.

22 (*a*) B. Mondal, M. G. Walawalkar and G. K. Lahiri, *J. Chem. Soc., Dalton Trans.*, 2000, 4209; (*b*) C. J. Cathey, E. C. Constable, M. J. Hannon, D. A. Tocher and M. D. Ward, *J. Chem. Soc., Chem. Commun.*, 1990, 621; (*c*) V. J. Catalano, R. A. Heck, C. E. Immoos, A. Ohman and M. G. Hill, *Inorg. Chem.*, 1998, **37**, 2150.

23 M. B. Robin and P. Day, *Adv. Inorg. Chem. Radiochem.*, 1967, **10**, 247.
24 B. K. Santra and G. K. Lahiri, *J. Chem. Soc., Dalton Trans.*, 1998, 139.
25 P. Bandyopadhyay, P. K. Mascharak and A. Chakravorty, *J. Chem. Soc., Dalton Trans.*, 1982, 675.
26 H. Bock, D. Z. Jaculi and B. Naturforsch, *Anorg. Chem. Org. Chem.*, 1991, **46**, 1091.
27 (*a*) B. K. Ghosh and A. Chakravorty, *Coord. Chem. Rev.*, 1989, **95**, 239; (*b*) V. R. L. Constantino, H. E. Toma, L. F. C. de Oliveira, F. N. Rein, R. C. Rocha and D. de O. Silva, *J. Chem. Soc., Dalton Trans.*, 1999, 1735.
28 (*a*) Z. Shirin and K. Mukherjee, *Polyhedron*, 1992, **11**, 2625; (*b*) K. S. Murray, A. M. van der Bergen and B. O. West, *Aust. J. Chem.*, 1978, **31**, 203; (*c*) G. S. Rodman and J. K. Nagle, *Inorg. Chim. Acta*, 1985, **105**, 205.
29 The Hush formula (see ref. 30) for calculation of the electronic coupling V_{ab} from the parameters of an IVCT process is: $V_{ab} = [2.05 \times 10^{-2}(\varepsilon_{max}\bar{\nu}_{max}\Delta\bar{\nu}_{1/2})^{1/2}]/R$ where ε_{max}, $\bar{\nu}_{max}$ and $\Delta\bar{\nu}_{1/2}$ are the molar extinction coefficient ($dm^3\ mol^{-1}\ cm^{-1}$), the absorption maximum (in wavenumbers), and the bandwidth at half maximum height (in wavenumbers), respectively; and R is the metal–metal distance in Å [taken as 6.57 Å from the average of the two Ru ··· Ru separations in the crystal structure of **[4]**$(ClO_4)_2$, see main text].
30 N. S. Hush, *Coord. Chem. Rev.*, 1985, **64**, 135.
31 R. W. Callahan, F. R. Keene, T. J. Meyer and D. J. Salmon, *J. Am. Chem. Soc.*, 1977, **99**, 1064.
32 (*a*) N. C. Fletcher, T. C. Robinson, A. Behrendt, J. C. Jeffery, Z. R. Reeves and M. D. Ward, *J. Chem. Soc., Dalton Trans.*, 1999, 2999; (*b*) A. K. Ghosh, S.-M. Peng, R. L. Paul, M. D. Ward and S. Goswami, *J. Chem. Soc., Dalton Trans.*, 2001, 336; (*c*) P. R. Auburn and A. B. P. Lever, *Inorg. Chem.*, 1990, **29**, 2551; (*d*) G. A. Heath, L. J. Yellowlees and P. S. Braterman, *Chem. Phys. Lett.*, 1982, **92**, 646.
33 M. D. Ward, *Inorg. Chem.*, 1996, **35**, 1712.
34 D. T. Sawyer, A. Sobkowiak and J. L. Roberts, Jr., *Electrochemistry for Chemists*, Wiley, New York, 1995.
35 S.-M. Lee, R. Kowallick, M. Marcaccio, J. A. McCleverty and M. D. Ward, *J. Chem. Soc., Dalton Trans.*, 1998, 3443.
36 G. M. Sheldrick, SADABS: A program for absorption correction with the Siemens SMART system, University of Gottingen, Germany, 1996.
37 SHELXTL program system version 5.1, Bruker Analytical X-Ray Instruments Inc., Madison, WI, 1998.